JACS
JOURNAL OF THE AMERICAN CHEMICAL SOCIETY
Article
pubs.acs.org/JACS

Probing the Molecular Origin of Native-State Flexibility in Repeat Proteins

Sharona S. Cohen,[†] Inbal Riven,[†] Aitziber L. Cortajarena,[‡] Lucia De Rosa,[§] Luca D. D'Andrea,[§] Lynne Regan,[∥] and Gilad Haran*[,†]

[†]Chemical Physics Department, Weizmann institute of Science, Rehovot 76100, Israel

[‡]IMDEA Nanociencia, CNB-CSIC-IMDEA Nanociencia Associated Unit "Unidad de Nanobiotecnología", Ciudad Universitaria de Cantoblanco, 28049 Madrid, Spain

[§]Istituto di Biostrutture e Bioimmagini, Consiglio Nazionale delle Ricerche, via Mezzocannone 16, 80134 Napoli, Italy

[∥]Molecular Biophysics & Biochemistry, Yale University, New Haven, Connecticut 06520, United States

Supporting Information

ABSTRACT: In contrast to globular proteins, the structure of repeat proteins is dominated by a regular set of short-range interactions. This property may confer on the native state of such proteins significant elasticity. We probe the molecular origin of the spring-like behavior of repeat proteins using a designed tetratricopeptide repeat protein with three repeat units (CTPR3). Single-molecule fluorescence studies of variants of the protein with FRET pairs at different positions show a continuous expansion of the folded state of CTPR3 at low concentrations of a chemical denaturant, preceding the all-or-none transition to the unfolded state. This remarkable native-state expansion can be explained quantitatively by a reduction in the spring constant of the structure. Circular dichroism and tryptophan fluorescence spectroscopy further show that the expansion does not involve either unwinding of CTPR3 helices or unraveling of interactions within repeats. These findings point to hydrophobic inter-repeat contacts as the source of the elasticity of repeat proteins.

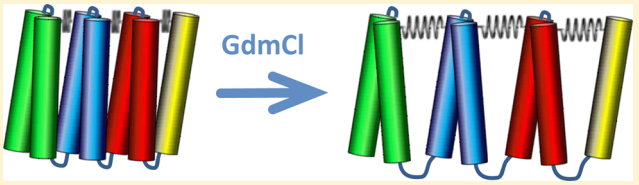

INTRODUCTION

Repeat proteins (RPs) are composed of tandem arrays of small structural units of 20−40 amino acids and often produce extended superhelical, solenoid-like structures.[1−3] RPs account for more than 5% of the proteins in the multicellular organism category of the Swiss-Prot database and are involved in a myriad of essential biological processes. In contrast to the complex and irregular tertiary structures of globular proteins, the tertiary structures of RPs are simple and modular. These structures involve extensive intra- and inter-repeat local contacts, but essentially no long-range interactions along their sequence.[4] The nonglobular structures of RPs result in large surfaces, which suit very well their function as recognition elements for different binding partners.[5,6]

Experiments and simulations on RPs suggest a significant level of structural flexibility,[7−10] in that their native structures accommodate substantial but reversible spring-like deformations. For example, atomic force microscopy experiments showed that an ankyrin repeat protein incurs a linear, spring-like extension at low forces preceding the unfolding transition.[7] In addition, several studies probed the elasticity of HEAT-repeat proteins, formed of helix−turn−helix repeat units. Molecular dynamics (MD) simulations of the 15 HEAT repeat containing protein, PR65, showed that it undergoes elastic deformations in response to pulling at its ends.[9] Flexibility in the tertiary structure of importin-β, another HEAT-repeat protein, was revealed by small-angle X-ray scattering experiments and MD simulations.[10,11] It is important to note that while some studies showed that at intermediate force levels individual repeat units of some repeat proteins unfolded,[12−14] the work cited above focuses on spring-like deformations that do not involve any unraveling of repeat units.

Interestingly, simulations suggested that the native-state flexibility of repeat proteins might be the result of an unusual malleability of inter-repeat contacts.[11] However, there is no experimental evidence to support this proposition. In this work we set to probe the molecular origin of repeat-protein flexibility. We reasoned that at denaturant concentrations that precede unfolding, this flexibility might be perturbed, and the effective spring constant of the protein would be lowered. We performed single-molecule FRET (smFRET) and other experiments on a protein comprising tandem units of the tetratricopeptide repeat (TPR) protein.[15]

The TPR motif is a 34 residue helix−turn−helix structure.[16] A consensus sequence of TPR, called CTPR and based on the sequence alignment of many individual TPR motifs, was introduced some time ago.[4] Proteins with different numbers of tandem CTPR units were studied extensively.[17−21] Our experiments were performed on a protein comprising three

Received: June 13, 2015
Published: July 24, 2015

DOI: 10.1021/jacs.5b06160
J. Am. Chem. Soc. 2015, 137, 10367−10373

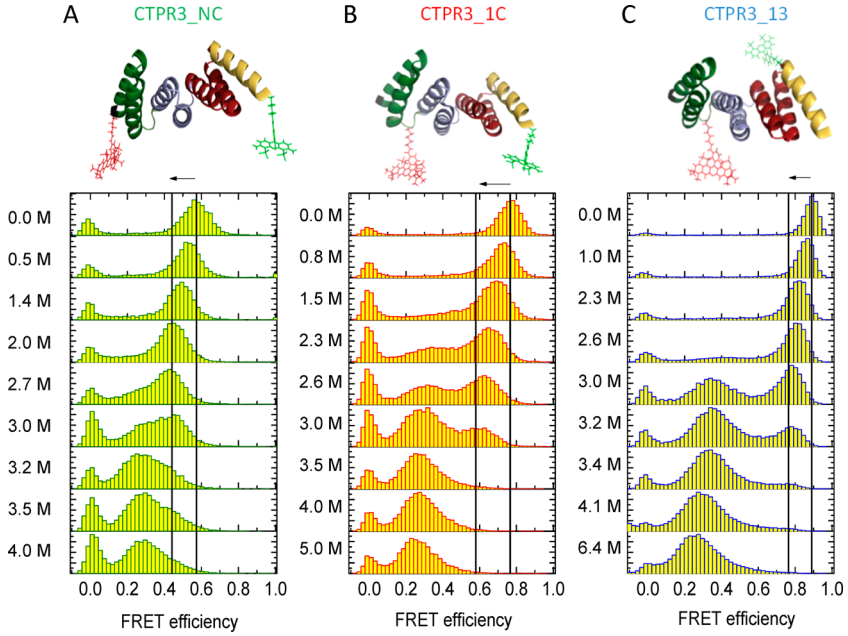

Figure 1. FRET histograms show a shift of the native-state peaks. FRET histograms of CTPR3_NC (A), CTPR3_1C (B), and CTPR3_13 (C), calculated from fluorescence bursts of diffusing molecules, are shown over a range of GdmCl concentrations, indicated to the left. The vertical lines designate the positions of the folded state peaks in the histograms under native conditions and at the maximal shift. The structure of each variant with the fluorescent dyes attached (donor in green and acceptor in red) is shown on top of each set of histograms. (The structure of CTPR3 is based on PDB file 1NA0.)

tandem repeats of the consensus TPR sequence, CTPR3. Three protein variants were prepared for smFRET studies, each double-labeled with fluorescent dyes for FRET (Figure 1). Experiments on freely diffusing molecules were conducted over a series of concentrations of the chemical denaturant guanidinum chloride (GdmCl). In all three labeled CTPR3 variants we observed a similar continuous decrease of the FRET efficiency of the folded state at low denaturant concentrations, preceding the unfolding transition of the protein. The change in FRET efficiency was attributed to a global expansion of the folded structure, which can be modeled as gradual weakening of the spring constant of the solenoid structure. Independent fluorescence correlation spectroscopy (FCS) measurements supported the same conclusion. Combined with a lack of change in circular dichroism spectra, as well as in the fluorescence spectra of the intrarepeat tryptophan residues of CTPR3, these results strongly implicate inter-repeat contacts (which are weakened here by the chemical denaturant) as the molecular origin of the flexibility of repeat proteins.

EXPERIMENTAL SECTION

Protein Labeling. CTPR3 expression and labeling was reported previously[22] and is described in some detail in the Supporting Information. In brief, we used a synthetic strategy based on expressed protein ligation, which allowed us to split the protein into two fragments. The N-terminal CTPR3 protein fragment (residues 1−104 in the case of CTPR3_13 and residues 1−120 in the case of CTPR3_NC and CTPR3_1C) was prepared as a C-terminal thioester derivative using intein technology. It was selectively labeled on its single cysteine residue (placed at the N-terminus in the case of CTPR3_NC or at position 36 in the case of CTPR3_1C and CTPR3_13) upon reaction with a probe containing a maleimide group. A native chemical ligation (NCL) reaction between the monolabeled thioester fragment and the C-terminal fragment afforded the full-length monolabeled protein. In the case of the CTPR3_13 variant, the C-terminal fragment consisted of a synthetic peptide corresponding to residues 105−120 and starting with a cysteine. In the case of the variants CTPR3_NC and CTPR3_1C, instead, NCL was performed with L-cysteine. The NCL reaction provided an additional cysteine in the full protein, which was finally exploited to introduce the second probe.

Single-Molecule Measurements. A home-built microscope described elsewhere[23] was used for single-molecule data acquisition, including FCS. For details see Supporting Information.

RESULTS AND DISCUSSION

GdmCl-Dependent smFRET Histograms of CTPR3. We perturbed the structure of the CTPR3 protein variants using the chemical denaturant GdmCl and measured the response using single-molecule FRET spectroscopy. CTPR3 is made of three helix−turn−helix repeats, plus an additional solvating helix at the C terminus.[4] Three double-labeled constructs of the protein were prepared, with the labeling sites varied systematically (Figure 1): (1) Acceptor (Alexa 594) at the N terminus, donor (Alexa 488) at the C terminus (CTPR3_NC); (2) Acceptor between the first and second repeats, donor at the C terminus (CTPR3_1C); and (3) Acceptor between the first and second repeats, donor between the third repeat and the solvating helix (CTPR3_13). Expressed protein ligation methodology was used to ensure 100% specific insertion of the donor and acceptor dyes at the desired positions.[22] This method completely avoids any heterogeneity in the results due to mixed locations of the dyes. Thus, the donor is always located at the labeling site closer to the C terminus and the acceptor at the site closer to the N terminus of the protein. It should be pointed out that, while the first two constructs involve helices at the N or C termini of the protein, in CTPR3_13 the dyes span only "internal" helices.

Double-labeled protein molecules were allowed to diffuse through the focus of a laser beam within a confocal microscope, and their fluorescence was registered on a photon-by-photon basis. Fluorescence bursts were identified in the measured data

DOI: 10.1021/jacs.5b06160
J. Am. Chem. Soc. 2015, 137, 10367−10373

sets (see Supporting Information) and were used to calculate the FRET efficiency value of each molecule. A histogram was constructed from the whole series of values. The measurement was repeated over a broad range of GdmCl concentrations. Observation of the whole set of histograms (Figure 1) suggested three populations of molecules: (1) A population at a high FRET efficiency value, due to the native, folded state of the protein. We will refer to this peak in the histograms as the "native-state peak". The center FRET efficiency of this peak was 44−89%, depending on the position of the donor−acceptor pair in a given construct and was in agreement with the crystal structure of CTPR3. (2) A population at a low FRET efficiency value (20−35%), due to the unfolded state. (3) A population with zero FRET efficiency, involving molecules in which only the donor fluorophore is activated.

All three constructs, irrespective of labeling positions, showed the same behavior: The native-state peak gradually shifted to lower FRET efficiency values over a range of denaturant concentrations at which the unfolded state was still not populated. The native-state peak of CTPR3 also shifted when urea was used as chemical denaturant (Figure S1). This behavior is very different from that of similarly sized globular proteins, which typically fold/unfold in a two-state process with only FRET peaks corresponding to the folded or unfolded state evident.[24−27] An example of the denaturation-associated FRET efficiency histograms of a globular two-state folding protein (protein L) is shown in Figure S2. No such gradual change in the FRET efficiency of the native state is observed. The gradual shift of the FRET efficiency of the folded state of CTPR3 was also evident in ensemble FRET measurements: the folded baseline of the denaturation curve was sloped (Figure S3). A series of control measurements allowed us to rule out the possibility that the shift in the histograms is due to changes in the properties of the dyes with respect to the denaturant concentrations (Figure S4, and also Supporting Information text).

To quantify the change in FRET efficiencies of the native-state peak, the histograms were fitted to three Gaussian distributions. The center values of the native-state peak at different GdmCl concentrations are shown in Figure 2A. These values were initially converted to distances under the assumption of a very narrow distance distribution (see Supporting Information for details). Distance changes relative to native conditions are plotted in Figure 2B, showing a similar trend for all variants, irrespective of the dye positions.

We used a simple spring model in order to fit the experimental data (See Supporting Information Text). The spring constant governs the width of the interdye distance distribution in this model, and the FRET efficiency is calculated from this distribution. The model predicts a reduction in mean FRET efficiency as the spring constant decreases, due to distribution broadening. Assuming that the spring constant depends exponentially on denaturant concentration allows us to fit the experimental data. The fits are shown as continuous lines in Figure 2A, and the spring constant values as a function of denaturant concentration are plotted in Figure S8. At 0 M GdmCl the spring constants obtained from the fit are 40 ± 9, 19 ± 4, and 11 ± 2 pN/nm for CTPR3_13, CTPR3_1C, and CTPR3_NC, respectively. The spring constant weakens as the distance between dyes increases.

The above analysis indicates that a spring-like behavior of the protein at low denaturant concentrations explains well our experimental results. Yet, there is a possibility that the shift of

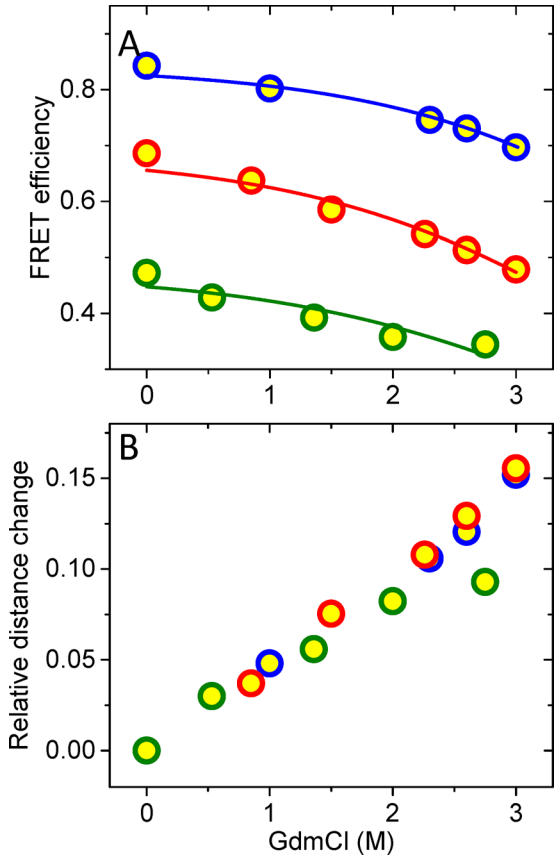

Figure 2. FRET efficiency values and interdye distances of CTPR3 variants. (A) Mean FRET efficiency values extracted from the native-state peaks in figure after correction for donor−acceptor quantum yield and detection efficiency differences. The continuous lines are fits to the spring model introduced in the Results and Discussion section. (B) Relative changes in interdye distances with respect to the distance at 0 M GdmCl, calculated from the values in panel A assuming very narrow distance distributions. (See Supporting Information for calculation details.) Green, CTPR3_NC; red, CTPR3_1C; and blue, CTPR3_13.

the folded-state peaks in the FRET efficiency histograms rather involves folding intermediates of the protein. In the next section we provide decisive evidence that this is not the case.

The FRET Efficiency Shift Cannot Be Attributed to Folding Intermediates. Previous studies of CTPR variants showed that their folding can be described by an Ising model, in which individual helices serve as interacting "Ising spins".[17] The model predicts that close to the denaturation transition midpoint there is a significant population of intermediates states (~20%), which are characterized by unraveling of end helices (while the central helices remain intact). However, at the low denaturant concentrations where native-state peak shifts are seen in the current work, the concentration of folding intermediates is predicted to be very small. This observation was borne out by analysis of native-state hydrogen exchange experiments.[19] Furthermore, we observe native-state peak shifts even for central helices (i.e., in the CTPR3_13 construct), while only the end helices are involved in the Ising intermediates. Thus, it is unlikely that the native-state peak shifts involve folding intermediates. Here we provide further experimental proof for this conclusion.

Let us assume that, in contrast to the discussion in the previous paragraph, there is an intermediate state that is

DOI: 10.1021/jacs.5b06160
J. Am. Chem. Soc. 2015, 137, 10367−10373

significantly populated even at the low denaturant concentration range relevant here. The contribution of this putative intermediate state to the FRET histograms might mix with the folded-state contribution. In this case the shape of the native-state peaks in the histograms would be dependent on the FRET efficiency of the intermediate as well as on the exchange rate between the intermediate and the folded state. We consider first the case that the exchange rate is much slower than the diffusion time of protein molecules through the laser beam, of the order of 1 ms. In this case, the probability of a transition between the states during the passage in the beam is small, and therefore each fluorescent burst would be due to a molecule in either of the two states. However, if the FRET efficiency values of the two states are close to each other, they would overlap and might lead to what would look like a single state, whose position would be a linear function of the position of the two original states. To test this possibility, we attempted to fit the native-state peak globally in each series of histograms assuming the FRET efficiency and peak width of one state is identical to that of the protein at 0 M denaturant, and the FRET efficiency and peak width of the second state is similar to that of the most shifted value of the distribution. The data could not be fitted by this model, because the distribution is too narrow at denaturant concentrations between the two extremes (See sample fits to CTPR3_1C data in Figure 3A, and fits to all three sets of histograms in Figure S5). Thus, we conclude that the shifting distribution is not due to two slowly interconverting states.

We further verified this observation with the following experiment. We measured FRET trajectories from CTPR3 molecules encapsulated in surface-tethered 100 nm lipid vesicles,[23,28,29] in the presence of GdmCl at intermediate concentrations. This experiment allowed us to probe transitions between states on a longer time scale, not limited by the diffusion time of the proteins. We found no evidence for transitions between two states in any of the many hundreds of trajectories measured (see more details in the Supporting Information).

One could still hypothesize that the exchange rate between the folded state and putative intermediate state is on the same time scale of the diffusion of molecules through the laser beam or even faster. Such a fast exchange between the two states may result in partial or full merging of the corresponding FRET efficiency distributions. This phenomenon is similar to the familiar "motional narrowing" scenario in spectroscopy and has been discussed by several groups, based on both theory and experiment.[30−32] Analysis using the Gopich−Szabo theory of ref 30 suggested that to account for the observed shape of the FRET efficiency distributions the exchange dynamics should be on a time scale much faster than a millisecond, indeed as fast as 10 μs (data not shown).

In order to identify such fast dynamics involving transitions between the folded state and the putative intermediate we used FRET FCS. In particular, the time-dependent cross-correlation function of donor and acceptor fluorescence intensities was measured. Fast exchange between two states with differing FRET efficiency values should manifest itself in the cross-correlation function as a phase that rises with time.[33−36] Using the formalism of ref 33, we estimated the amplitude of the rising phase. Based on the FRET efficiency of the folded state of CTPR3_1C (0.77) and the FRET efficiency of its putative intermediate (which we set equal to the FRET efficiency of the most shifted distribution, 0.57), this amplitude should be at least ∼0.04.

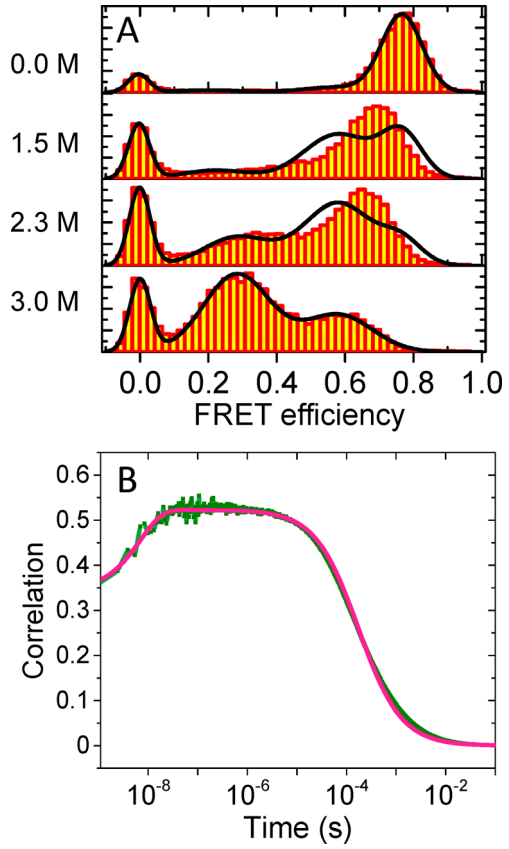

Figure 3. The shifting peaks in the histograms cannot be explained as averages of two populations. (A) Fits of the CTPR3_1C histograms from Figure 1, assuming that the folded-state interchanges slowly with an intermediate state, whose FRET efficiency is identified with the most shifted position of the native-state peak in the histograms. Clearly the fits fail to capture the shape of the peaks in the histograms at intermediate GdmCl concentrations. (B) Donor−acceptor intensity cross correlation of CTPR3_1C measured at 1.5 M GdmCl. The curve shows two dynamic phases: a rising phase at short times due to antibunching and a decaying phase at long times due to diffusion. At intermediate times the curve is essentially flat, and no additional rising phase due to conformational dynamics is seen, ruling out fast exchange between the folded state and a putative intermediate.

The experimental donor−acceptor intensity cross-correlation function was calculated from measurements on molecules of CTPR3_1C in 1.5 M GdmCl and is shown in Figure 3B. At the longest times the curve shows a decaying phase that is due to diffusion of the molecules through the laser beam, while at the shortest times there is a rising phase due to antibunching (reflecting the inability of the dyes to be excited again while already in the excited state).[37] At intermediate times the curve is essentially flat, and no additional rising phase due to conformational dynamics is seen. Since the noise characteristics of these measurements should have allowed us to readily observe a rising phase with an amplitude of ∼0.04 as predicted above, we can exclude fast exchange between the folded state and an intermediate state.

The above correlation analysis is limited to time scales faster than the diffusion times of molecules through the laser beam (a few hundred microseconds). We calculated donor−acceptor intensity cross-correlation function also from the trajectories of immobilized molecules. This correlation function, discussed in the Supporting Information and presented in Figure S9, is not

DOI: 10.1021/jacs.5b06160
J. Am. Chem. Soc. 2015, 137, 10367−10373

limited by diffusion. It is also found to be flat, now up to a time scale of a few milliseconds, extending the observation of a lack of fast exchange between the folded state and an intermediate state.

As indicated above, the analysis in this section shows that the shift of the folded-state FRET efficiency histogram must be due to an effective expansion of the protein structure at low denaturant concentrations.

Photoinduced Electron-Transfer Fluorescence Correlation Spectroscopy. In order to independently verify the finding of a gradual expansion of the folded state of CTPR3, we performed a series of FCS experiments on CTPR3 molecules labeled at the C terminus with the donor dye (Alexa 488) only. It is well-known that many fluorescent dyes are quenched, either dynamically or statically, by aromatic side-chains.[38,39] Static quenching involves transient formation of a ground-state complex between a dye molecule and an aromatic side-chain. Illumination of the complex leads to photoinduced electron transfer that quenches the dye. The signature of the formation of such a complex in the autocorrelation curve is a decaying phase, whose time constant depends on the distance of the dye from the quencher. Thus, using these measurements one can follow distance changes due to expansion.

Curves measured at a series of GdmCl concentrations are shown in Figure 4A. At the earliest times we see the antibunching phase. Following this phase the curve shows a sequence of decaying phases. The decaying phase on the longest time scale is due to the overall diffusion of the protein, as above. Preceding it is a phase due to triplet dynamics, as can be deduced by its sensitivity to laser power.[40] The fastest decaying phase can be attributed to complex formation between the dye and aromatic residues of the protein.

When there is a significant separation of time scales between the complex formation dynamics and triplet dynamics, it is possible to model the decaying phase in a relatively straightforward manner. Indeed, in this case the rate constant of the phase due to complex formation becomes the sum of the association and dissociation rates, and its amplitude is the ratio of these two rates.[41,42] The association rate depends on the relative time it takes the dye and the quenching side-chain to diffuse toward each other and hence may report on the conformation of a protein.[42,43]

The complex association and dissociation rates as a function of GdmCl concentration were calculated from fits to the autocorrelation curves of Figure 4A and are shown in Figure 4B. We find that as the GdmCl concentration increases, the complex association rate decreases by up to five times compared to native conditions, while at the same time the dissociation rate remains almost constant. The complex association rate can be modeled as involving the diffusion of the dye until it collides with the quenching aromatic side chain and therefore depends on the effective diffusion coefficient and the distribution of distances between the colliding partners.[42] Since the increase in GdmCl concentration over the range 0–1.5 M should not significantly affect viscosity, and hence chain diffusion, it is reasonable to assign the decrease of the association rate to an increased average distance between the complex-forming partners, perhaps combined with reduced accessibility due to the conformational change incurred by the molecule. The weak dependence of the dissociation rate on GdmCl concentration is in agreement with previous studies from our lab.[42] This set of measurements therefore supports

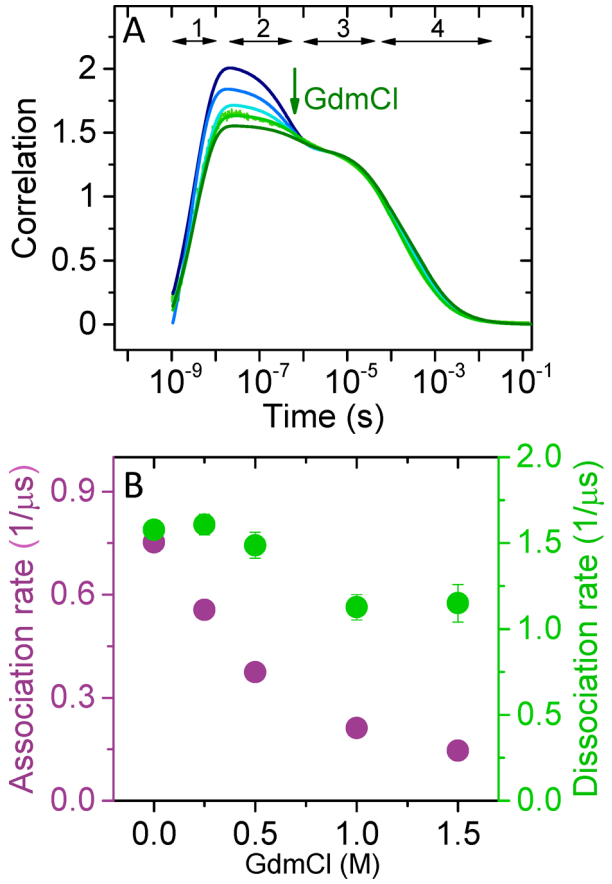

Figure 4. FCS corroborates expansion of the folded state. (A) Intensity autocorrelation functions of CTPR3 labeled with Alexa 488 at the C terminus measured over a range of GdmCl concentrations (0, 0.25, 0.5, 1, 1.5 M) at which only the native-state peak is populated. Four phases are observed and marked on the figure. Phase 1 corresponds to antibunching; phase 2 is due to complex formation of the dye with its quencher and reports on folded-state expansion; phase 3 is a result of triplet-state dynamics; and phase 4 is due to diffusion of the molecules through the laser focus. (B) Rates of association and dissociation of the complex between dye and quencher extracted from fits to the autocorrelation functions. The association rate decreases significantly with GdmCl, supporting native-state expansion.

our finding of a gradual expansion of the protein observed by smFRET experiments.

Ensemble Spectroscopy of CTPR3. To obtain more information as to which parts of the structure of CTPR3 participate in the expansion observed by the smFRET experiments, we used tryptophan fluorescence spectroscopy. Each repeat of CTPR3 contains one tryptophan residue, whose side chain partially packs between the two helices of the repeat in the folded structure. Fluorescence emission spectra measured as a function of denaturant concentration showed essentially no change in either peak position (Figure 5A) or intensity in the range 0–2.5 M. The fluorescence anisotropy also did not change over this range. These findings indicate that over this range of GdmCl concentration the intrarepeat structure remains intact.

This conclusion is corroborated by circular dichroism spectroscopy, which shows no loss of helical structure before the unfolding transition (Figure S6). Hence the expansion observed in FRET histograms is most likely a result of inter-repeat structural changes. To probe whether hydrophobic side

DOI: 10.1021/jacs.5b06160
J. Am. Chem. Soc. 2015, 137, 10367–10373

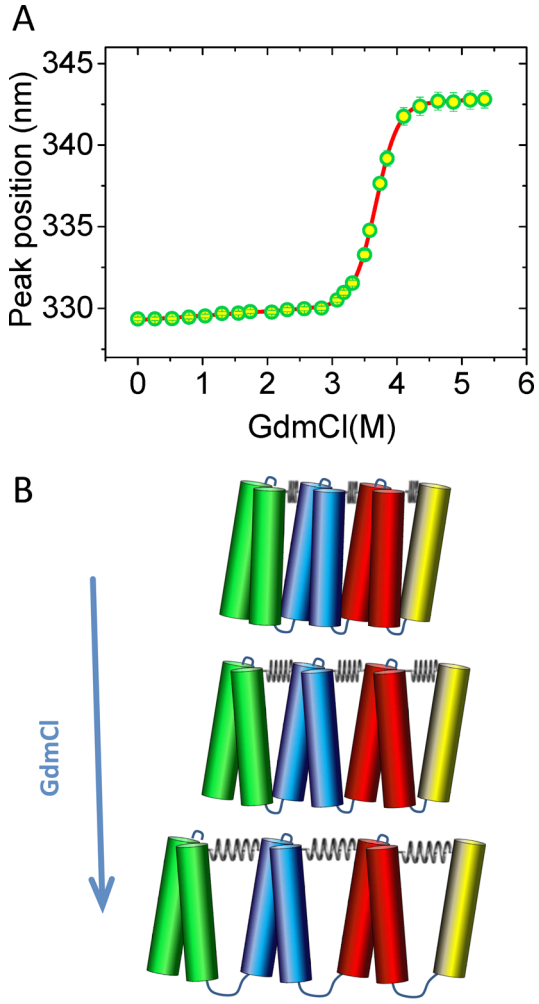

Figure 5. Inter-repeat rather than intrarepeat interactions are weakened by denaturants. (A) Fluorescence emission spectra of tryptophan residues, which are located within the repeat units CTPR3, remain unchanged up to 2.5 M GdmCl. The peak position as a function of denaturant concentration is shown. The blue line is a sigmoidal curve fit, including linear baselines. The essential lack of change up to 2.5 M GdmCl indicates that tryptophan residues are not exposed to water. (B) The effect of denaturants can be modeled as an effective reduction of the spring constant of the molecule due to modulation of inter-repeat hydrophobic contacts. The spring constant reduction and concomitant broadening of the distance distribution lead to an apparent gradual expansion of the native-state peaks in FRET efficiency histograms.

chains residing between repeats get exposed to the solvent during the expansion, we performed experiments with the hydrophobic dye 8-anilino-1-naphthalenesulfonic acid. No fluorescence increase was observed over the same range of denaturant concentration as above (Figure S7), indicating that hydrophobic side chains remain buried even as the structure of inter-repeat regions gets modulated. A similar phenomenon was observed by Kappel et al.[11] in their simulations.

CONCLUSION

The main finding of this work is the expansion of the folded state of CTPR3 at low denaturant concentrations, preceding the main unfolding transition. We found this expansion both from smFRET histograms and FCS experiments. In conjunction with a lack of change in tryptophan fluorescence and CD spectra, our experiments point to a variation of the interaction between neighboring repeats rather than structural changes within repeats. The gradual expansion of folded CTPR3 points to relatively weak hydrophoboic interactions between its repeats which are progressively weakened as the denaturant concentration is increased.[11] Our work thus naturally connects to the literature discussing the elasticity of RPs.[9,44]

As already pointed out in the Introduction section, multiple RPs undergo reversible structural changes in response to forces that are smaller than those required for complete unfolding. It was suggested that these proteins can be classified as soft springs, with a spring constant in the range ∼2−20 pN/nm. Such soft springs incur significant end-to-end fluctuations. The spring constants obtained from a fit of a spring model to our experimental data are of the same order of magnitude as above. They decrease as the denaturant concentration is increased, pointing to weakening of the CTPR3 spring as the reason for the reduced FRET efficiency (Figure 5B). And since we have determined that the denaturant-induced changes involve inter-repeat contacts, this implies that these contacts constitute the origin of the elasticity of this repeat protein. There is a growing consensus in current literature that chemical denaturants function through dispersion interactions with hydrophobic groups.[45] A modulation of the hydrophobic inter-repeat contacts without significant exposure to the solvent, as seems to be the case here, is reminiscent of the dry molten globule phenomenon, which was recently observed experimentally.[46,47] The involvement of the inter-repeat interfaces in the spring-like motion of CTPR3 might be further tested by mutations of residues in these regions; however, this is complicated by the fact that all such mutations are also expected to change the overall stability of the protein.

This work thus sheds experimental light on the molecular basis for the elasticity of RPs in general and TPRs in particular, demonstrating that it can be modulated by weakening hydrophobic interactions at the interfaces between repeat units, therefore connecting single-molecule force spectroscopy and FRET experiments. It has been proposed that forced unfolding differs significantly from chemical denaturation due to the formation of very extended conformations in the former.[48] This difference is less relevant to the low force−low denaturant concentration regime discussed here, and indeed both force measurements and our own experiments lead to a similar range of values for the spring constants.

How CTPR3 looks when the inter-repeat contacts are weakened remains to be determined. It has been shown that pulling on HEAT-repeat proteins reduces their curvature.[9,11] TPR proteins have a spiral staircase-like structure, which originates in the significant twist experienced by each repeat as it packs to its neighbors.[15] It is possible that this twist is gradually relieved by the addition of denaturants, making the protein more expanded and less solenoidal. As a final point we will mention an interesting issue that remains open, which is the relationship between the "spring-like" behavior and the function of repeat proteins within the cell.[3,10] Future work will shed light on these open questions.

ASSOCIATED CONTENT

Supporting Information

The Supporting Information is available free of charge on the ACS Publications website at DOI: 10.1021/jacs.5b06160.

DOI: 10.1021/jacs.5b06160
J. Am. Chem. Soc. 2015, 137, 10367−10373

(Additional experimental details, supporting experiments and analyses as well as supporting figures PDF)

AUTHOR INFORMATION

Corresponding Author

*gilad.haran@weizmann.ac.il

Notes

The authors declare no competing financial interest.

ACKNOWLEDGMENTS

This work was partly funded by a grant from the Human Frontier Science Program (to L.R., G.H., and L.D'A.). G.H. is the incumbent of the Hilda Pomeraniec Memorial Professorial Chair. He also acknowledges partial support from the Minerva foundation with funding from the Federal German Ministry for Education and Research and from the Israel Science Foundation through grant no. 686/14. L.R. acknowledges the support of the Raymond and Beverly Sackler Institute for Biological, Physical and Engineering Science. We thank Hagen Hofmann, Simon Mochrie and Menahem Pirchi for insightful discussions, Marcus Jäger for providing the protein L plasmid, and Claus Seidel for usage of his program FPS for the calculation of inter-dye distances.

REFERENCES

(1) Javadi, Y.; Itzhaki, L. S. *Curr. Opin. Struct. Biol.* **2013**, *23*, 622.
(2) Andrade, M. A.; Perez-Iratxeta, C.; Ponting, C. P. *J. Struct. Biol.* **2001**, *134*, 117.
(3) Kobe, B.; Kajava, A. V. *Trends Biochem. Sci.* **2000**, *25*, 509.
(4) Main, E. R. G.; Jackson, S. E.; Regan, L. *Curr. Opin. Struct. Biol.* **2003**, *13*, 482.
(5) Bjorklund, A. K.; Ekman, D.; Elofsson, A. *PLoS Comput. Biol.* **2006**, *2*, e114.
(6) Grove, T. Z.; Cortajarena, A. L.; Regan, L. *Curr. Opin. Struct. Biol.* **2008**, *18*, 507.
(7) Lee, G.; Abdi, K.; Jiang, Y.; Michaely, P.; Bennett, V.; Marszalek, P. E. *Nature* **2006**, *440*, 246.
(8) Sotomayor, M.; Schulten, K. *Science* **2007**, *316*, 1144.
(9) Grinthal, A.; Adamovic, I.; Weiner, B.; Karplus, M.; Kleckner, N. *Proc. Natl. Acad. Sci. U. S. A.* **2010**, *107*, 2467.
(10) Forwood, J. K.; Lange, A.; Zachariae, U.; Marfori, M.; Preast, C.; Grubmuller, H.; Stewart, M.; Corbett, A. H.; Kobe, B. *Structure* **2010**, *18*, 1171.
(11) Kappel, C.; Zachariae, U.; Dolker, N.; Grubmuller, H. *Biophys. J.* **2010**, *99*, 1596.
(12) Li, L.; Wetzel, S.; Pluckthun, A.; Fernandez, J. M. *Biophys. J.* **2006**, *90*, L30.
(13) Serquera, D.; Lee, W.; Settanni, G.; Marszalek, P. E.; Paci, E.; Itzhaki, L. S. *Biophys. J.* **2010**, *98*, 1294.
(14) Settanni, G.; Serquera, D.; Marszalek, P. E.; Paci, E.; Itzhaki, L. S. *PLoS Comput. Biol.* **2013**, *9*, e1002864.
(15) Main, E. R.; Xiong, Y.; Cocco, M. J.; D'Andrea, L.; Regan, L. *Structure* **2003**, *11*, 497.
(16) Goebl, M.; Yanagida, M. *Trends Biochem. Sci.* **1991**, *16*, 173.
(17) Kajander, T.; Cortajarena, A. L.; Main, E. R.; Mochrie, S. G.; Regan, L. *J. Am. Chem. Soc.* **2005**, *127*, 10188.
(18) Main, E. R.; Stott, K.; Jackson, S. E.; Regan, L. *Proc. Natl. Acad. Sci. U. S. A.* **2005**, *102*, 5721.
(19) Cortajarena, A. L.; Mochrie, S. G.; Regan, L. *J. Mol. Biol.* **2008**, *379*, 617.
(20) Javadi, Y.; Main, E. R. *Proc. Natl. Acad. Sci. U. S. A.* **2009**, *106*, 17383.
(21) Cortajarena, A. L.; Mochrie, S. G. J.; Regan, L. *Protein Sci.* **2011**, *20*, 1042.
(22) De Rosa, L.; Cortajarena, A. L.; Romanelli, A.; Regan, L.; D'Andrea, L. D. *Org. Biomol. Chem.* **2012**, *10*, 273.
(23) Pirchi, M.; Ziv, G.; Riven, I.; Cohen, S. S.; Zohar, N.; Barak, Y.; Haran, G. *Nat. Commun.* **2011**, *2*, 493.
(24) Sherman, E.; Haran, G. *Proc. Natl. Acad. Sci. U. S. A.* **2006**, *103*, 11539.
(25) Merchant, K. A.; Best, R. B.; Louis, J. M.; Gopich, I. V.; Eaton, W. A. *Proc. Natl. Acad. Sci. U. S. A.* **2007**, *104*, 1528.
(26) Hoffmann, A.; Kane, A.; Nettels, D.; Hertzog, D. E.; Baumgartel, P.; Lengefeld, J.; Reichardt, G.; Horsley, D. A.; Seckler, R.; Bakajin, O.; Schuler, B. *Proc. Natl. Acad. Sci. U. S. A.* **2007**, *104*, 105.
(27) Pugh, S. D.; Gell, C.; Smith, D. A.; Radford, S. E.; Brockwell, D. J. *J. Mol. Biol.* **2010**, *398*, 132.
(28) Boukobza, E.; Sonnenfeld, A.; Haran, G. *J. Phys. Chem. B* **2001**, *105*, 12165.
(29) Rhoades, E.; Gussakovsky, E.; Haran, G. *Proc. Natl. Acad. Sci. U. S. A.* **2003**, *100*, 7418.
(30) Gopich, I. V.; Szabo, A. *J. Phys. Chem. B* **2010**, *114*, 15221.
(31) Chung, H. S.; Gopich, I. V.; McHale, K.; Cellmer, T.; Louis, J. M.; Eaton, W. A. *J. Phys. Chem. A* **2011**, *115*, 3642.
(32) Yang, H. *Cell Signaling Reactions: Single-Molecular Kinetic Analysis*, 1st ed.; Yasushi, S., Masahiro, U., Eds.; Springer: The Netherlands, 2011; pp 199.
(33) Torres, T.; Levitus, M. *J. Phys. Chem. B* **2007**, *111*, 7392.
(34) Price, E. S.; DeVore, M. S.; Johnson, C. K. *J. Phys. Chem. B* **2010**, *114*, 5895.
(35) Margittai, M.; Widengren, J.; Schweinberger, E.; Schroder, G. F.; Felekyan, S.; Haustein, E.; Konig, M.; Fasshauer, D.; Grubmuller, H.; Jahn, R.; Seidel, C. A. P *Proc. Natl. Acad. Sci. U. S. A.* **2003**, *100*, 15516.
(36) Chung, H. S.; Louis, J. M.; Eaton, W. A. *Proc. Natl. Acad. Sci. U. S. A.* **2009**, *106*, 11837.
(37) Kask, P.; Piksarv, P.; Mets, U. *Eur. Biophys. J.* **1985**, *12*, 163.
(38) Chen, H.; Ahsan, S. S.; Santiago-Berrios, M. B.; Abruna, H. D.; Webb, W. W. *J. Am. Chem. Soc.* **2010**, *132*, 7244.
(39) Doose, S.; Neuweiler, H.; Sauer, M. *ChemPhysChem* **2005**, *6*, 2277.
(40) Widengren, J.; Rigler, R.; Mets, U. *J. Fluoresc.* **1994**, *4*, 255.
(41) Widengren, J.; Dapprich, J.; Rigler, R. *Chem. Phys.* **1997**, *216*, 417.
(42) Sherman, E.; Haran, G. *ChemPhysChem* **2011**, *12*, 696.
(43) Neuweiler, H.; Doose, S.; Sauer, M. *Proc. Natl. Acad. Sci. U. S. A.* **2005**, *102*, 16650.
(44) Dembinski, H.; Wismer, K.; Balasubramaniam, D.; Gonzalez, H. A.; Alverdi, V.; Iakoucheva, L. M.; Komives, E. A. *Phys. Chem. Chem. Phys.* **2014**, *16*, 6480.
(45) England, J. L.; Haran, G. *Annu. Rev. Phys. Chem.* **2011**, *62*, 257.
(46) Jha, S. K.; Udgaonkar, J. B. *Proc. Natl. Acad. Sci. U. S. A.* **2009**, *106*, 12289.
(47) Reiner, A.; Henklein, P.; Kiefhaber, T. *Proc. Natl. Acad. Sci. U. S. A.* **2010**, *107*, 4955.
(48) Stirnemann, G.; Kang, S. G.; Zhou, R.; Berne, B. J. *Proc. Natl. Acad. Sci. U. S. A.* **2014**, *111*, 3413.

DOI: 10.1021/jacs.5b06160
J. Am. Chem. Soc. 2015, 137, 10367−10373